

PACS numbers: 42.62.Eh; 42.55.Lt; 42.60.Da; 06.30.Bp
DOI: 10.1070/QE2000v030n02ABEH001675

Development of new methods and means of dynamic laser goniometry

M N Burnashev, D P Luk'yanov, P A Pavlov, Yu V Filatov

Abstract. **The methods and instruments of dynamic laser goniometry developed over many years of research carried out in the St Petersburg State Electrotechnical University [formerly Leningrad Electrotechnical Institute (LETI)] are considered. The primary sources of error and conditions for error minimisation are identified and evaluated. The laser goniometers developed have been used to certify optical polygons and angular position sensors, to estimate angular motion parameters of various objects, and specifically to measure angular positions of crystals in the unique diffraction spectrometer built at the St Petersburg Institute of Nuclear Physics (PINP) of the Russian Academy of Sciences. Modern measurement technologies combined with a self-calibrated ring laser allowed a large amount of measuring information to be accumulated over a short (1 to 5 min) period of time and ensured that the random component of angle measurement uncertainty is as small as 0.02 to 0.03″ in the 0 – 360° range. On the basis of inertial properties of a ring laser, a new concept was proposed for constructing a new generation of measuring systems intended to estimate complex angular motions and to provide dynamic calibration of multiple-axis test beds, large-scale antenna systems, telescopes, and other objects.**

1. Introduction

Dynamic laser goniometry has evolved into a separate scientific subdivision where the fundamental properties of a ring-cavity laser are used to develop and apply fast high-precision automated systems for plane angle measurements [1 – 5]. The proposal to use a ring laser (RL) in the goniometer was put forward for the first time in the French patent [1] in 1968. The first dynamic laser goniometer (DLG) with a measurement uncertainty of 0.5″ was developed at the All-Union Mendeleev Research Institute of Metrology (VNIIM) in the late 1970s [2]. The Arsenal Plant in Kiev manufactured the first commercial laser goniometer, GS-1L, at the beginning of the 1980s in cooperation with LETI [3, 4]. At the present time, this system is used as the angle standard at the Metrology Institute of Slovakia (Bratislava) [5]. Further investigations were and are being carried out at the St Petersburg State Electrotechnical University (SPSETU) [6 – 8].

M N Burnashev, D P Luk'yanov, P A Pavlov, Yu V Filatov St Petersburg Electrotechnical University, 5 ul. Professora Popova, 197376 St Petersburg, Russia

Received 30 June 1999
Kvantovaya Elektronika **30** (2) 141 – 146 (2000)
Translated by Yu A Atanov, edited by L Dwivedi

Dynamic goniometry, featuring a RL continuously rotating with constant angular velocity, provides the most favourable conditions for attaining very high precision and for executing periodic self-calibrations against the natural standard of 2π plane angle. In its turn, the self-calibration calls for the development of special instruments for fixing the dynamic reference directions defining standard angle values. Such an instrument, called the zero-indicator (ZI), has to provide an accuracy close to that of the RL. In our work we prefer to use a ZI based on the double-reflecting interferometer with integral fringe-pattern recording [3, 9]. When an RL with a scale factor of about 10^6 is used, high resolution can be achieved by applying interpolators based either on frequency multiplication of the RL output signal or on interpolation of a fraction of the signal period.

The measurement technologies applied in modern dynamic laser goniometry allow one to evaluate its potential capabilities limited by quantum fluctuations of the RL output signal, equal to a few thousandths of an angular second.

2. Generalised diagram of DLG

The basic principles of dynamic laser goniometry can be illustrated by considering a goniometer designed for certification of optical polygons (OP). Fig. 1 shows a ring laser (1) mounted along with an OP (4) on a rotor (2). The angular velocity of the rotor is chosen such that RL operation corresponds to the linear part of the output characteristic (i.e., far from the lock-in zone). The ZI (5), which forms a parallel light beam and registers the moments of time at which a subsequent face is located at right angles to the beam, is fixed to the stationary base of the goniometer.

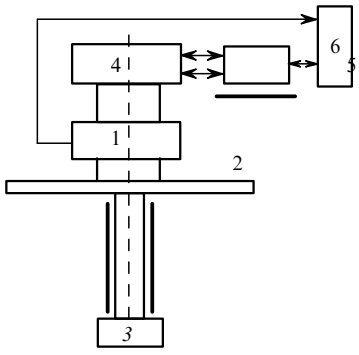

Figure 1. Generalised diagram of a DLG: (1) RL; (2) Goniometer rotor; (3) Drive; (4) OP; (5) ZI; (6) Computer interface.

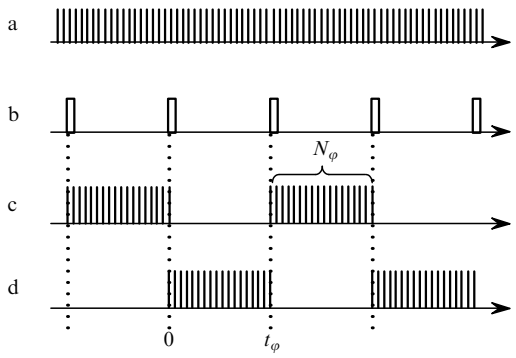

Figure 2. DLG output signals: RL pulses U_{RL} (a) and ZI pulses U_{ZI} (b); results of pulse summation by counters C_1 and C_2 (c) and (d).

The output signals from the RL and ZI are directed via an interface (6) to the computer for further processing. These are illustrated in Fig. 2. The oscillogram of Fig. 2a shows the formed sequence of RL pulses whose number within the measurement interval $0 - t_\varphi$ is determined by the expression

$$N_\varphi = \int_0^{t_\varphi} K\Omega \cos\alpha \, \mathrm{d}t = \varphi K \cos\alpha \ , \tag{1}$$

where $K \approx 4S/\lambda L$ is the RL scale factor; S and L are the area and perimeter of the RL resonator; λ is the wavelength; φ is the rotation angle over the interval $0 - t_\varphi$; α is the angle between the angular velocity vector $\boldsymbol{\Omega}$ and the RL measurement axis. Hereafter we shall assume that $\cos\alpha \approx 1$. If the measurement system applies the interpolation with interpolation factor n, then the scale factor in Eqn (1) has to be replaced by Kn.

The oscillogram of Fig. 2b shows the ZI pulses whose number per rotor revolution is equal to the number of polygon faces. The counters C_1 and C_2 sum the pulses of the RL output occurring between neighbouring ZI pulses in two channels, respectively (Figs 2c, 2d). To reduce the effects of drift of the RL scale factor, self-calibration over the complete revolution has been provided (by using the natural standard of the 2π plane angle)

$$N_{2\pi} = \int_0^T K\Omega \, \mathrm{d}t = 2\pi K \ , \tag{2}$$

where T is the duration of one revolution. Using Eqns (1) and (2), one obtains the measured angle as

$$\varphi = 2\pi \frac{N_\varphi}{N_{2\pi}} \ . \tag{3}$$

3. Correlation analysis of random measurement error

Using Eqns (1) and (2), we can represent the summing of pulses (1) and (2):

$$N(t) = N^0(t) + \delta N(t) \ ,$$

where $N^0(t)$ is a linear time function and $\delta N(t)$ is a non-stationary random process characterising the measurement uncertainty. The function $\delta N(t)$ can be subdivided into two components. The first is caused by contribution from the broadband fluctuations $\delta\omega(t)$ of the frequency of the RL output signal. It can be written as

$$\delta N^{\omega}(t) = \frac{1}{2\pi} \int_0^t \delta\omega(t') \, \mathrm{d}t' \ . \tag{4}$$

The second component is defined by the ZI errors, which result in variations of the limits of integration of the RL signal:

$$\delta N^t(t) = K \left[\int_t^{t+\delta t(t)} \Omega(t') \mathrm{d}t' - \int_0^{\delta t(0)} \Omega(t') \mathrm{d}t' \right]$$

$$= \frac{N_{2\pi}}{2\pi} [\Omega(t)\delta t(t) - \Omega(0)\delta t(0)]. \tag{5}$$

Finally, we obtain $\delta N(t)$ as the sum

$$\delta N(t) = \delta N^{\omega}(t) + \delta N^t(t) \ .$$

Neglecting intermediate calculations of angle measurement errors via the correlation functions $R_N^{\omega}(t_1, t_2)$ and $R_N^t(t_1, t_2)$ of the random processes $\delta N^{\omega}(t)$ and $\delta N^t(t)$ and assuming the white noise model for frequency fluctuations of the RL output signal, we shall obtain, on the basis of Ref. [10], the final expression for the random uncertainty of angle measurement (see Fig. 3):

$$D_\varphi(\varphi) = \begin{cases} 2D_\varphi^t + \left(r_{\mathrm{w}}^2 T - 2D_\varphi^t\right) \dfrac{\varphi}{2\pi} \left(1 - \dfrac{\varphi}{2\pi}\right), & \varphi \neq 0 \, , \, 2\pi, \\ D_\varphi(\varphi) = 0 \, , & \varphi = 0, \, 2\pi, \end{cases} \tag{6}$$

where $D_\varphi^t = (2\pi/T)^2 D^t = 0.0009''(\text{ang. sec.})^2$; D^t is the variance of moments of registering the angle borders; $r_{\mathrm{w}}^2 T - 2D_\varphi^t = 0.0013''(\text{ang. sec.})^2$; and $r_{\mathrm{w}} = 0.05''/c^{1/2}$ is the coefficient of the random RL drift.

It is seen from these results that the maximum variance does not exceed $0.0024''(\text{ang. sec.})^2$, i. e., the standard deviation $\sigma < 0.05''$. Further reduction of uncertainty in DLG is realised via reading and statistical processing of large amounts of measurement data, which can easily be performed in the real-time regime.

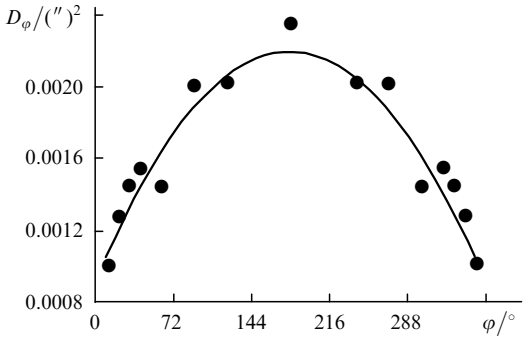

Figure 3. DLG uncertainty as a function of the measured angle; calculated from Eqn 6 (line), experimental values (dots).

4. Calibration of angle encoders

Calibration of discrete angle encoders, such as photoelectric and magnetic encoders, inductosyns, etc., as well as angle standards (optical polygons, limbs, and so on), was the basic problem for whose solution the first DLG was developed. As an example, let us consider the goniometer IUP-1L developed at the SPETU and intended for precision calibrations of angle encoders of various types, contactless

measurements of the angular position of an 'external' object, and measurements of the angular velocity of a moving 'external' object. This goniometer has been put through elaborate metrological tests at PTB (Braunschweig, Germany) and compared against reference standards in VNIIM (St Petersburg, Russia) [7].

The schematic diagram of the IUP-1L is shown in Fig. 1 and its general appearance in Fig. 4. As a rule, the goniometer uses either the ring laser KM-11 manufactured by the Polyus research institute, or the laser GL-1 (Elektrooptika) [10, 11]. The ring laser with wavelength $\lambda = 0.63$ μm represents a cubic pyroceramic monoblock with prism reflectors and a perimeter of 44 cm. The active He – Ne medium is excited by a low-voltage high-frequency discharge. The RL scale factor amounts to ~ 1.3 arc sec pulse^{-1}, which corresponds to about one million pulses per revolution. To increase the resolution of the goniometer, the frequency multiplier of the RL output signal with multiplication coefficient 10 is used. The ring laser of the DLG is mounted on the rotor rotating at the velocity of about 0.7 rev s^{-1} with an instability of 0.5%.

5. Calibration of optical polygons

Figure 4. General view of the laser goniometer IUP-1L. The upper plate of the device supports a photoelectric angle encoder RON255 mounted ready for the calibration.

The OP calibrations are carried out by using the interference ZI [3, 9] built in the goniometer IUP-1L to ensure registration of the OP faces at normal directions during the process of measurement. The random measurement error in the OP calibrations is usually reduced by revolving the goniometer rotor for 50 to 100 revolutions (with the total time of measurements being 0.5 to 1.5 min). Conducting a series of such measurements reveals that the standard deviation of the results of each measurement from the mean value for the whole series is as low as $0.02 - 0.03''$. One of the sources of systematic uncertainty during OP calibrations is a tilt of the optical polygon with respect to the goniometer axis of rotation when ZI is tilted relative to its optical axis.

To exclude this uncertainty, cross calibration is usually performed [12], which consists of n measurement cycles (equal to the number of OP faces). After each cycle, the OP is turned through an angle $360^\circ/n$ relative to the goniometer rotor and the new measurement cycle is carried out. The

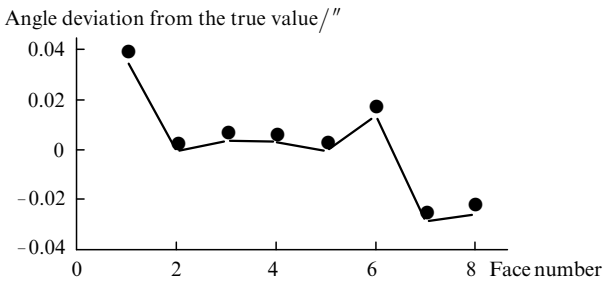

Figure 5. Comparison of calibration results for an 8-face polygon with the certification data obtained using the State standard of the plane angle (VNIIM).

overall calibration results for n angles of the OP are obtained by processing the $n \times n$ measurement matrix. As an example of use of the IUP-1L goniometer, in Fig. 5 some calibration results are shown for a standard octagonal prism certified by using the primary VNIIM standard [7]. One can see that the angle values obtained from calibrations with the IUP-1L goniometer do not deviate by more than $0.04''$ from the certification values.

6. Calibration of photoelectric angle encoders

In this case the calibrated photoelectric (optical) angle encoder (OAE) was mounted on the special platform of the goniometer in such a way that its axis of rotation coincided with the axis of rotation of the goniometer. If there was no need to calibrate all lines of the OAE, the frequency of the OAE output signal was divided in a ratio allowing sufficient discreteness of calibrated angular intervals. Using the IUP-1L goniometer, we calibrated various OAEs manufactured by the Heidenhain Co. (RON255, RON905, etc.), holographic encoders developed at the PINP, and code optical encoder prototypes produced by Avangard Co.

The calibration of a serial increment OAE RON255 for 12° intervals consisted of 25 measurements, each of which was made for 25 revolutions of the goniometer rotor. Fig. 6 illustrates how the results obtained in one measurement deviate from the mean value for the entire series of measurements. The standard deviation for the whole series equals $0.019''$ and characterises the reproducibility of measurement results obtained in calibrations of OAEs with the IUP-1L goniometer. The standard deviation (averaged over

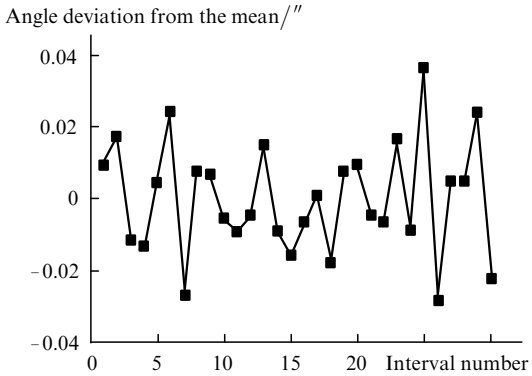

Figure 6. Deviations of measurement data from the mean value for the whole measurement series during the calibration of an RON255.

the entire series of measurements) for the cumulative error did not exceed 0.03″.

7. Inverted laser goniometer

The inverted laser goniometer (ILG) makes it possible to measure the angular position of various objects: test beds, apparatus for marking line standards of length, turn-tables used in physical experiments, and so on. In this layout, the goniometer rotor is positioned coaxially with the rotated object (Fig. 7). In addition to the RL (2), the goniometer rotor (1) features the ZI (4). The object (6) supports the inspection mirror (5) whose angular position with respect to the fixed reference mirror (3) is measured by the goniometer. The ZI rotating together with the goniometer rotor generates the pulses at the moments of time when its optical axis coincides with the normals to mirrors (3) and (5). As in the traditional goniometer layout, the intervals between the ZI pulses in the ILG are filled with the RL signal to allow measurements of the angular position of the object relative to the reference direction. In this case the range of measurements spans 360° while the measurement accuracy achieved is typical for laser goniometry.

The ILG was used together with a bicrystal diffraction spectrometer developed at the PINP [8]. Two samples were produced to correspond to the layout shown in Fig. 7. In this case the object of measurement was the rotating platform of the spectrometer with the crystal mounted on it. The investigations of the intensity of the $K_{\alpha 1}$ Mo x-ray line ($E = 17.47334$ keV, $\lambda = 71$ Å) showed that the random uncertainty of angular measurements was about 0.05″.

8. Contact-free measurement of angular position of an 'external' object

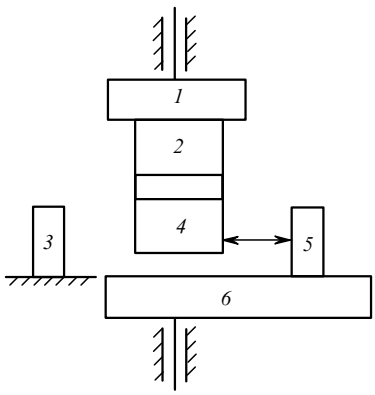

Figure 7. Schematic diagram of the ILG: (1) rotor; (2) RL; (3) reference mirror; (4) ZI; (5) inspection mirror; (6) measurement object.

There exist many problems involving measurements of angular positions of objects located at a distance (sometimes at a considerable distance) from a measurement device. Such problems are usually solved by using autocollimators or theodolites. These instruments have quite small measurement uncertainties (below 0.1″) in a very small angular range of few minutes of arc. A modified DLG layout makes it possible to make such angular measurements with high accuracy in the range from 20° to 30° [7, 14].

In this case an OP is applied for spatial scanning of the light beam from the ZI. The reference mirror is fixed to the goniometer base whereas the inspection mirror is mounted on the measurement object. The ZI generates pulses at the moments of time when its light beam scanned by the OP falls on both the reference and the inspection mirrors at right angles. The frequency f of measurements of the angular position of the investigated object is defined by the product of the rotation velocity Ω and the number n of the OP faces: $f = n\Omega/2\pi$. For large separations L of the inspection mirror from the DLG, the range $\Delta\varphi_{\max}$ of angular measurements depends on the diameter D of the investigated mirror and is equal to $2\arctan(D/2L)$. Therefore the measurement range exceeds 11° for the mirror diameter $D = 100$ mm and $L = 0.5$ m.

The metrological characteristics of the IUP-1L goniometer were studied in this operation regime by using the standard reference rotary table at PTB (Germany) [7], which provides angular positioning with an uncertainty of 0.1″ (1σ). The investigations were carried out for subsequent rotations of the table through 1° followed by measurements of the angular position of the table relative to the inspection mirror (4) by means of the IUP-1L goniometer. The results obtained showed that the step uncertainty is below 0.2″ the and cumulative uncertainty below 0.35″ throughout the measurement range equal to 24°.

The DLG was applied successfully to estimate the angular velocity of various moving objects. Specifically the accuracy of the high-precision rotary unit capable of reproducing the angular velocities in the range from 6×10^{-5} to 6 rad s^{-1} [15] was evaluated in 1990–92. By using a 72-face OP rotating with a velocity of $\sim$0.8 Hz we obtained a measurement frequency of about 58 Hz. In measurements of ultra-low velocities ($10^{-2} - 10^{-3}$ rad s^{-1}) with averaging over 1440 points, the uncertainty of angular velocity measurements was equal to 1.2×10^{-6} rad s^{-1}.

In 1993 the Aerospace Research Center (DLR, Braunschweig, Germany) evaluated the uncertainty of the inductosyn of the triple-axis Acutronic test bed by using the goniometer IUP-1L goniometer located at a distance of 1.7 m from the investigated reflector.

9. Concepts of a new generation of DLGs used to measure parameters of complex angular motions of objects

The DLG configurations described earlier were intended for operating on a stationary base and used the RL as a high-resolution angle transducer. However, the most fundamental property of the RL — its sensitivity to absolute angular velocity — was not utilised. New industrial technologies require fast high-precision measurements of complex angular motion of various objects, such as multiple-axis calibration stands, large-scale surveying antenna systems, optical telescopes, unique rotor devices, etc.

To check and certify these objects, the measuring systems are mounted directly on them, so that the angles, angular velocities, and angular accelerations are measured on a movable base in a wide dynamic range. This approach calls for a transition to a novel method of dynamic laser goniometry, where the inertial properties of the RL are utilised efficiently.

The concept of the method described can be reduced to a formation on the base of the rotating RL of the inertial frame of reference with respect to which the complex angular motion of the base is determined. The functional diagram

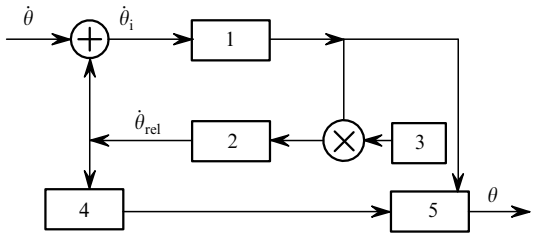

Figure 8. Functional diagram of the INLG: (1) RL; (2) drive; (3) reference oscillator; (4) OAE; (5) computer interface.

of the inertial laser goniometer (INLG) is shown in Fig. 8. The INLG rotor together with the RL (1) revolves with a constant angular velocity relative to inertial space. The goniometer features the OAE (4) making it possible to determine angular displacements of the INLG rotor with respect to its stator. The RL (1) and OAE (4) attached to the rotor measure the different angular quantities, i. e., the angular position of the rotor, $\theta_i(t)$, relative to the inertial space and the angular position of the rotor, $\theta_{rel}(t)$, relative to the stator.

Assuming that $\theta(t)$ denotes the angular position of the base, which performs a complex angular motion, we can write:

$$\dot\theta_i(t) = \dot\theta(t) + \dot\theta_{rel}(t) \ .$$

The phase stabilisation system (2) controls the motion of the INLG by comparing the signal from the RL (1) and the signal from the reference oscillator (3) operating at the frequency ω_0. This provides the rotation of the INLG rotor in inertial space with quasi-constant angular velocity at which the frequency of the RL output signal frequency varies insignificantly. The current angular position of the basis can be found from the previous relation as

$$\theta(t) = \theta_i(t) - \theta_{rel}(t) \ .$$

The kinematic diagram of the INLG is illustrated in Fig. 9. The ZI (1) and OP (2) are inserted into the ILG in order to ensure calibration of the scale factor of RL.

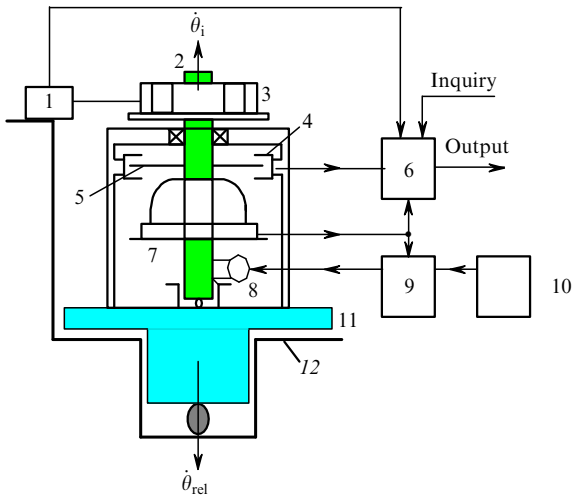

Figure 9. Kinematic diagram ofthe INLG: (1) ZI; (2) rotor; (3) OP; (4) OAE stator; (5) OAE rotor; (6) computer interface; (7) RL; (8) drive; (9) system for stabilisation of rotation velocity; (10) reference frequency oscillator; (11) rotating testbed; (12) stationary base.

10. Description of information-carrying INLG signals

In accordance with the INLG concept, the ring laser rotates in inertial space with nearly constant angular velocity and its output signal represents a harmonic oscillation at a quasi-constant frequency. In this case the dynamic parameters of motion of the object are determined almost wholly by the OAE. Its output signal varies in a wide dynamic range depending on the characteristics of motion. In this connection it seems relevant to consider the OAE signal parameters in more detail. Since the OAE signal can be expanded into a Fourier series of simple harmonic components, it is sufficient to examine the response of the sensor to the harmonic input of the following type:

$$\Theta_{rel} = \omega_0 t + \theta_m \sin(\Omega t + \Psi_m) + \theta_0 \ ,$$

where ω_0 is the angular velocity of the 'smooth' rotation of the rotor set by the reference oscillator of the servomotor; θ_m, Ω, and Ψ_m are the amplitude, frequency, and initial phase of angular oscillations of the object; and θ_0 is the initial angular position of the object. When the OAE transmission coefficient $k = N$, where N is the number of reference signals of the sensor per one revolution, the photodetector generates the following output signal:

$$U(t) = U_0 \sin k[\omega_0 t + \theta_m(\sin \Omega t + \Psi_m) + \varphi_0] \ ,$$

which represents the oscillation phase-modulated by a harmonic function. The spectrum of this signal can be represented as an expansion into an infinite series of Bessel functions [16]:

$$U(t) = U_0 \sum_{-\infty}^{\infty} J_n(k\theta_m) \cos[(k\omega_0 + n\Omega)t + n\Psi_m + k\varphi_0].$$

The tendency to use an OAE with higher resolution, e.g., a holographic encoder of angular displacements PKG-105M with the coefficient $k = 3.24 \times 10^5$, brings about an abrupt increase in the phase deviation $k\theta_m$, which in its turn causes spectral broadening of the photodetector output signal. Fig. 10 shows the signal spectrum for $k\theta_m = 5$. The frequency band occupied by the OAE output signal can be estimated from the expression

$$\Delta\omega \approx 2[1 + k(\theta_m \ddot\theta_m)^{1/2}] \ . \qquad (7)$$

By way of example, let us estimate the frequency band Δf of the OAE output signal for the following initial data typical of triple-axis test beds: $\theta_m = 120^\circ$, $\ddot\theta_m = 2500^\circ c^{-2}$. Inserting these values in Eqn (7), we obtain $\Delta f = \Delta\omega/2\pi \approx 1$ MHz at the modulation frequency $F = \Omega/2\pi \approx 0.73$ Hz. The values obtained for Δf and Ω suggest that the frequency band occupied by an OAE output signal contains $1.4 \times 10^6 \Delta f/F$ individual components, which allows approximation of the linear spectrum considered by a quasi-continuous one. To ensure undistorted reproduction of this spectrum, the bandwidth of the transmission path from the

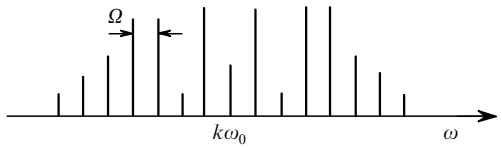

Figure 10. Spectrum of a phase-modulated OAE signal for $k\theta_m = 5$.

photodetector should satisfy the condition $f_{up} > f$, at which the amplitude and phase distortions are reduced to a minimum.

The complex character of the angular motions of test beds makes it necessary to estimate not only the amplitude distortions of the output signal, but also its time delays due to the phase – frequency characteristics. The complex analysis of dynamic errors introduced by the RL, optical sensor, and null indicator, results in a total ILG uncertainty of $\pm 0.19''$ up to angular velocities of $200^\circ\ s^{-1}$ at accelerations $2500^\circ\ s^{-2}$ and working frequencies up to 100 Hz. The deterministic character of dynamic suggests that they can be reduced via hardware-controlled and algorithmic methods.

11. Conclusions

Methods and instruments of dynamic laser goniometry have outgrown laboratory research and organically enhanced traditional angle-measurement technologies owing to their high-speed unlimited range of angular measurements, high precision, etc. DLG uncertainties as low as $0.02 - 0.03''$ were achieved for ring lasers of intermediate accuracy and for total internal reflection polygons.

Further increase in DLG accuracy is associated with the transition to more promising RL systems with multiple-layer dielectric mirrors, in which the losses can be reduced down to $(2-4)\times 10^{-6}$. The combination of such an RL with high-resolution holographic angle transducers will enable creation of a new national plane angle standard, whose development is at present being conducted jointly by the SPSETU, VNIIM, PINP, and others.

The need for measurement of complex angular motion parameters has led to the development of totally new DLG architecture, where both the high accuracy characteristics and the inertial properties of ring lasers have been utilised. This allows us to speak about the advent of a new scientific subdivision, inertial laser goniometry.

References

1. Catherin J M, Dessus B, French Patent No. 1511089 (granted 26.01.68)
2. Blanter V E, Filatov Yu V Metrologia (1) 3 (1979)
3. Batrakov A S., Butusov M M, Loukianov D P et al. Laser Measurement Systems (Moscow: Radio i Svyaz', 1981)
4. Vanyurikhin A I, Zaitsev I I Opt.-Mekh. Promst. (9) 28 (1982)
5. Mokros J, Vu K X Jemna Mech. Opt. **9** 203 (1993)
6. Loukianov D P, Pavlov P A, Filatov Yu V Gyro Technology Symposium (Stuttgart, Germany, 1991)
7. Filatov Yu V, Loukianov D P. Probst R Metrologia **34** 343 (1997)
8. Burnashev M N, Kirianov K E, Loukianov D P, Mezentsev A A, Filatov Yu V, Pavlov P A Meas. Sci. Technol. **9** 1067 (1998)
9. Filatov Yu V Opt.-Mekh. Promst. (4) 13 (1989)
10. Filatov Yu V., Loukianov D P., Pavlov P A., Burnashev M N Optical Gyros and their Application (RTO AGARDograph 339, 1999)
11. Kuryatov V N Proceedings of the Second International Conf. on Inertial Navigation, St Petersburg, Russia, 1995
12. Sim P J, in Modern Techniques in Metrology (Singapore: World Scientific, 1984) p. 102
13. Probst R VDI Reports (1118) 173 (1994)
14. Filatov Yu V., Loukianov D P., Pavlov P A VDI Reports (1118) 123 (1994)
15. Asaulenko P A., Shakhmatov A F Trudy LGTU (437) 35 (1992)
16. Karatyanu K Frequency Modulation (Bucharest: Academy of Sciences of Romanian People's Republic, 1961)